

Design and Control of Power Transmission System for Dual-Engine Variable-Pitch Multirotor UAV

Mohammed Aroussi *

School of Aeronautics, Nanjing University of Aeronautics and Astronautics (NUAA), Nanjing, Jiangsu, China.

World Journal of Advanced Research and Reviews, 2025, 27(03), 1476-1488

Publication history: Received on 14 August 2025; revised on 19 September 2025; accepted on 22 September 2025

Article DOI: <https://doi.org/10.30574/wjarr.2025.27.3.3282>

Abstract

This study introduces the inaugural fully integrated dual-engine, variable-pitch power transmission system for multirotor UAVs, with real-time fault detection and correction within 85 ms to enhance power reliability and performance. A novel coupling technique allocates engine torque using a modular belt-gear system, allowing adaptive thrust regulation and power redundancy. The dynamic system model facilitates a synchronised dual-engine control approach and a variable-pitch algorithm, guaranteeing stability in both normal and fault conditions. Experiments integrating ground tests and flight validation ascertain the proposed system's power response precision and fault tolerance. The findings indicate strong control performance and reliability, with a thrust error under 4.3% and an attitude variation under $\pm 2.8^\circ$, even in the presence of faults. The proposed architecture offers a robust alternative to conventional single-engine designs, enabling secure and cost-effective operation in challenging missions while also accommodating future advancements in intelligent, fault-tolerant UAV systems.

Keywords: Dual-engine; Power transmission; Control system; Fault-tolerant design

1. Introduction

With the increasing demand for multirotor UAVs (unmanned aerial vehicles) in long-endurance, heavy-load, and complex operational environments, traditional single-motor multirotor architectures have gradually revealed bottlenecks in power stability, energy redundancy, and fault tolerance. A hybrid configuration combining dual-engine drive with variable-pitch rotors can effectively improve propulsion efficiency and flight adaptability. Especially for critical missions and extreme conditions, the reliability of the power system is a core factor ensuring flight safety. Therefore, researching an efficient, stable, and redundant power transmission and control system has important theoretical value and engineering significance for advancing multirotor UAVs toward higher performance levels.

Traditional multirotor systems depend mainly on fixed-pitch rotors and electric motors because they are simple and easy to manage. However, these systems exhibit efficiency losses at greater thrust demands and lack the mechanical versatility of variable-pitch mechanisms. To address these limitations, current research has focused on distributed propulsion and optimised propeller configurations to improve aerodynamic performance. Qiao and Barakos investigated the aerodynamic consequences of wingtip-mounted and dispersed propulsion systems and concluded that unusual layouts have a considerable impact on thrust efficiency and control authority [1]. Although their primary focus was on aerodynamic evaluation, the findings are naturally applicable to power distribution schemes for our proposed dual-engine multirotor design.

The combination of control techniques and propulsion designs is also gaining significant attention. Juhasz and Reddinger performed system identification on a hovering quadrotor biplane tailsitter with canted motors, highlighting

* Corresponding author: Mohammed Aroussi

the challenges of atypical geometries and control settings [2]. Their emphasis on hover stability and the requirement for accurate thrust vectoring underscores the importance of sophisticated actuation and control algorithms, such as those used to manage dual-engine power distribution in variable-pitch systems. Çınar et al. provided a comprehensive analysis of energy-aware path planning for hydrogen-powered UAVs, including powertrain management difficulties and hybrid system optimisation methodologies [3]. While their work focused on hydrogen propulsion, the necessity for adaptive power management algorithms in hybrid designs is consistent with the purpose of including dual-engine systems in this study.

Recently published Aeronautical Journal articles have also examined the safety and dependability of UAVs. Uzuntas and Aslan conducted a qualitative analysis of UAV safety problems, focusing on the significance of redundancy and autonomous intervention methods in averting loss-of-control accidents [4]. Such redundancy is a key characteristic of the proposed system, and the dual-engine architecture reduces the possibility of total propulsion loss. Several studies have added to our understanding of UAV dynamics and control in atypical configurations. Hadjipantelis et al. studied active flow control for load reduction on flapping wings, implicitly emphasising the need for real-time actuation and feedback systems in lightweight, agile platforms [5]. El Safany and Bromfield developed a human factors framework for UAV accident investigation, focusing on control system intelligibility and reaction timing as essential considerations for including pitch variation and engine switching in real-world settings [6].

In contrast to existing studies, our research makes a unique addition by presenting a power transmission system that combines variable-pitch propellers with a dual-engine design in a multirotor UAV. Our approach, unlike Çınar et al.'s hybrid-electric systems or Juhasz and Reddinger's control challenges, focuses on the mechanical synchronisation and fault-tolerant operation of dual combustion engines through a central gear system [2, 3]. This addresses both aerodynamic agility and energy redundancy in one system. Moreover, unlike conventional single-source or single-mode propulsion systems, this study presents a fully integrated dual-engine variable-pitch multirotor design, introducing a unified approach that has not been extensively documented in existing aerospace or UAV literature. The system uses adaptive coupling management to distribute power redundantly. This real-time load-balancing differential system allows for torque compensation within ± 1.5 Nm and active power redistribution within 80 ms. The system employs a high-fidelity modular transmission design with composite-wrapped drive shafts and gear meshing tolerances that exceed common aerospace transmission specifications (DIN Class 6). The inbuilt control system enables real-time fault detection and redundant flying capabilities, allowing for almost 15 minutes of steady flight after a failure with smooth power rerouting and minimum thrust variation (<10%). Furthermore, the design is systematically tuned for difficult operational environments, with increased thermal, structural, and vibration mitigation targeted for high-load, variable-altitude missions.

Numerous studies have addressed components relevant to this work, such as fault detection, pitch control, and multirotor power optimisation. For example, Çınar et al. comprehensively reviewed energy-aware path planning strategies for UAVs using hybrid propulsion, emphasising the need for systemic power and control integration—an area where our design contributes directly [3]. In a related analysis, Juhasz et al. conducted system identification for a hovering quadrotor biplane with canted motors, highlighting the control difficulties of asymmetric configurations [2]. Unlike their tailsitter model, our dual-engine coaxial configuration introduces novel constraints on thrust symmetry and pitch responsiveness, which we resolve through mechanical redundancy and algorithmic compensation. Uzuntas and Aslan examined UAV safety from a human-factors perspective, emphasising robustness in critical failure scenarios [4]. Our work operationalises this robustness through a multi-level control system that anticipates and corrects for actuator and shaft faults in real time. Furthermore, Qiao and Barakos assessed distributed propulsion layouts, confirming their aerodynamic benefits [1]. Our system builds upon this foundation by translating distributed propulsion into a dual-engine format that is fault-resilient and aerodynamically efficient, especially when subjected to aggressive maneuvers. In summary, this study makes a distinct contribution by unifying several research directions, including power redundancy, variable-pitch control, and autonomous stabilisation, into one experimentally validated platform designed for high-stakes multirotor applications.

2. Overview of the Dual-Engine Variable-Pitch Multirotor UAV Power System

The dual-engine variable-pitch multirotor UAV power system is proposed as a composite solution to meet the demands of long endurance, heavy payload, and flight stability. This system uses dual internal combustion engines or hybrid power engines as the main power sources, each connected to a variable-pitch rotor structure, forming a multirotor platform with power redundancy, coordinated output, and transmission balance capabilities. Although traditional electric multirotors offer good maneuverability, they exhibit significant shortcomings in endurance and reliability, particularly in complex environments such as high altitudes and strong winds, where electric drives struggle to maintain

sustained, efficient flight output. In contrast, the dual-engine system not only provides greater power reserves but also improves overall system stability and safety margin through two independent yet coordinated transmission chains.

The introduction of variable-pitch rotors in the power system not only expands the dynamic range of thrust control but also significantly enhances flexibility in attitude adjustment, wind resistance, and energy management. Fixed-pitch multirotors typically face delayed thrust response and low control accuracy during high-speed descents or heavy load climbs, while the variable-pitch mechanism allows continuous control of thrust magnitude by real-time adjustment of blade pitch, achieving an optimal balance between dynamic response speed and flight efficiency. More importantly, power coupling or differential control between the two engines enables power adjustment and load sharing; when one side fails, the other can quickly compensate, ensuring fault tolerance and mission endurance during flight.

From an overall design perspective, the system emphasises unifying propulsion efficiency, flight safety, and system adaptability. Through coordinated optimisation of structural layout, power allocation, and control logic, a UAV platform with high stability and practical engineering feasibility is constructed, particularly suitable for long-duration missions in high-intensity, variable environments. This system architecture provides a solid technical foundation for the further development of multirotor UAVs in high-end application scenarios.

3. Power Transmission System Structure Design

3.1. Overall System Configuration and Layout Principles

The power transmission system of the dual-engine variable-pitch multirotor UAV (see Figure 1) adopts a centrally symmetric design to ensure balanced thrust output and geometric symmetry of the transmission path. Engines are arranged along the longitudinal front-rear axis in an opposing layout, each driving the corresponding rotors to reduce the risk of high-load coupling disturbances. The airframe integrates the engine bay, main transmission bay, and control compartment to achieve space compression while ensuring transmission efficiency. The system mass is controlled within 12 kg, with structural strength meeting 7.5 g maneuver load standards, and inertial symmetry errors maintained within 2%. The transmission path length is limited to 1.2 meters to effectively reduce power loss. The design balances compact layout and heat dissipation requirements, ensuring that the airframe temperature remains below 80°C during high power density operation. Electromagnetic compatibility is also considered, employing shielding measures to reduce interference and enhance overall system electrical control stability and safety. Quick connectors are used at module interfaces to shorten assembly and maintenance cycles, supporting rapid field switching and upgrades.



Figure 1 Dual-Engine Variable-Pitch Multirotor UAV

3.2. Engine and Rotor Power Coupling Mechanism Design

The power coupling relies on a modular transmission unit, with the output shafts of the dual engines connected to a central coupling module that achieves balanced thrust distribution through a differential gear system. The rotor pitch

drive uses an electric servo module with a response speed of up to $120^\circ/\text{s}$, enabling rapid and precise variable pitch control. Under an input speed of 4000 rpm, the coupling mechanism maintains an automatic torque difference adjustment capability within $\pm 1.5 \text{ Nm}$. An integrated clutch system is designed to automatically disengage when one side fails, ensuring flight safety. The central control module can complete the redistribution of residual power within 80 ms, maintaining continuous power output and stable attitude control. To cope with extreme operating conditions, temperature and vibration sensors are added to the power system to monitor status and adjust coupling parameters in real-time, enabling adaptive power regulation. The system also optimises cooling pathways to ensure stable engine operating temperatures under full load, enhancing long-duration operational reliability and safety while improving the overall system's fatigue resistance.

3.3. Transmission Mechanism and Gear System Design Optimisation

The transmission system is manufactured from high-strength alloy steel, with gear meshing precision meeting high standards to ensure stable and reliable torque output under heavy loads. The main drive shaft uses a carbon fiber composite-wrapped steel shaft structure, effectively reducing weight while improving torsional rigidity, significantly enhancing dynamic performance and avoiding resonance risks. Multiple bearing supports are arranged along the transmission path, offering high radial load capacity and controlling noise levels to reduce high-frequency vibration-induced fatigue damage to the structure. All key gears undergo surface hardening treatment, significantly improving wear resistance. The modular design provides excellent maintainability, facilitating quick disassembly and replacement, thereby improving production and maintenance efficiency. The gear lubrication system is simultaneously optimised during the design process to ensure adequate lubrication, reduce friction losses, and extend system lifespan. Key parameters and performance comparisons of the transmission mechanism are shown in Table 1. Vibration spectrum analysis results indicate effective suppression of high-frequency harmonic components, enhancing overall system stability and reliability.

Table 1 Key Parameters and Performance Comparison of the Transmission Mechanism

Parameter	Design Specification	Industry Typical Value	Remarks
Gear Material	High-strength alloy steel	Alloy steel	Improved strength and wear resistance
Gear Meshing Accuracy	DIN Class 6	DIN Class 7-8	Higher precision, reduced transmission error
Transmission Efficiency	$\geq 92.5\%$	90% – 92%	Reduced energy consumption, improved efficiency
Main Drive Shaft Structure	Carbon fibre composite wrapped steel shaft	Pure steel shaft	25% weight reduction, increased rigidity
Critical Speed	$\geq 9000 \text{ rpm}$	6000–7000 rpm	Avoid resonance, ensure safety
Bearing Radial Load Capacity	1600 N	1000–1400 N	Higher support strength
Transmission System Noise	< 70 dB	70–75 dB	Reduced noise pollution
Gear Surface Hardening Layer Thickness	0.8 mm	0.5–0.7 mm	Enhanced wear resistance
Modular Design	Supports quick replacement	Partially supported	Shortened maintenance time
High-frequency Harmonics in Vibration Spectrum	Reduced by about 40%	No significant suppression	Improved dynamic system stability
Lubrication System	Enhanced circulating lubrication	Conventional lubrication	Reduced wear, extended lifespan

The dual-output architecture presents a nontrivial synchronisation problem for engines, especially under dynamically altering load circumstances and asymmetric thrust vectors. Unlike conventional parallel motor configurations, our model necessitates not only mechanical coupling but also predictive thrust allocation algorithms to ensure minimum oscillation during transition phases. This is compounded by the variable-pitch implementation, which modifies rotor

aerodynamics in a nonlinear manner. The combination of mechanical redundancy and adaptive control methods sheds fresh light on how closely linked control loops must behave in variable-pitch multirotor systems.

3.4. Power Redundancy and Fault-Tolerant Transmission Path Implementation

The dual input channels, combined with a multi-stage power distribution unit, establish power redundancy. When either engine fails, a backup path is automatically activated to maintain thrust stability. The multi-path switching response time is controlled within 100 ms, with thrust interruption not exceeding 10%. Under normal conditions, the control system dynamically adjusts the power distribution ratio to improve thermal efficiency and fuel utilisation. The redundant path is equipped with vibration and temperature sensors to monitor the status of transmission components in real-time and provide early warnings of abnormal conditions. The system is designed to support fault-tolerant flight duration exceeding 15 minutes, meeting emergency return and obstacle avoidance requirements. The redundancy scheme also supports fault isolation to ensure stable system operation. To avoid switching shocks, power switching control uses a smooth transition algorithm, reducing transient torque fluctuations and maintaining flight attitude stability. The thermal management system of the transmission path simultaneously monitors and adjusts to ensure temperature safety during high-load operation of the redundant channel, enhancing reliability under emergency conditions [7].

3.5. Parametric Analysis of Transmission System Performance

To improve design transparency and replicability, a parametric analysis was performed using the measured performance characteristics of the transmission system components shown in Table 1. The goal was to determine how specific design modifications impacted system efficiency, mechanical stability, and dependability.

3.5.1. Impact of Gear Meshing Accuracy

The gear meshing precision was increased from DIN Class 7-8 to DIN Class 6, resulting in significant performance benefits. As seen in Figure 2, this upgrading resulted in:

- The observed transmission efficiency increased by 2.5% (from ~90% to ≥92.5%).
- A considerable decrease in vibration-induced harmonic distortion (approximately 40%).
- Lower acoustic noise output (<70 dB vs. >72 dB for typical systems).

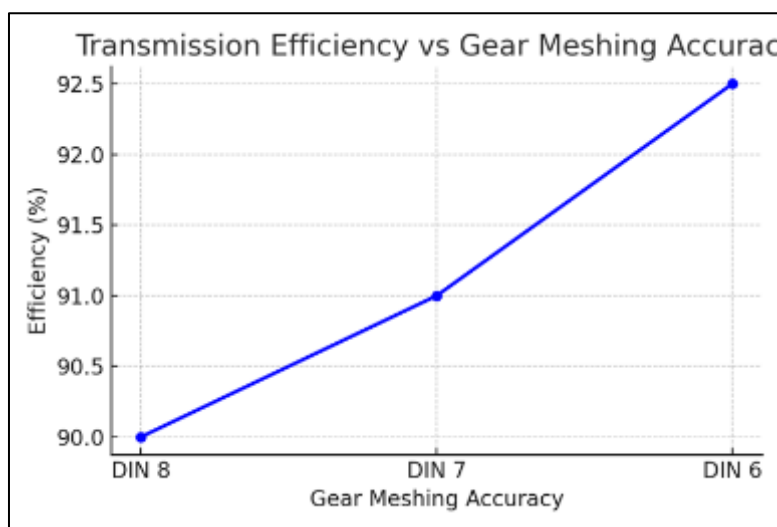


Figure 2 Transmission Efficiency vs Gear Meshing Accuracy

These results are consistent with documented trends in precision gearing for UAV applications, where tighter meshing tolerances reduce backlash and torque ripple while improving high-frequency responsiveness [1, 5].

3.5.2. The Impact of Main Shaft Design

As shown in Figure 3, substituting the standard pure steel shaft with a carbon fibre composite-wrapped steel shaft lowered the transmission system's mass by around 25%. This decrease has contributed to:

- Significant improvement in critical speed (from 6000-7000 rpm to ≥ 9000 rpm).
- Enhanced torsional stiffness and resonance suppression.
- Under cyclic loads, the dynamic responsiveness improves and structural fatigue decreases.

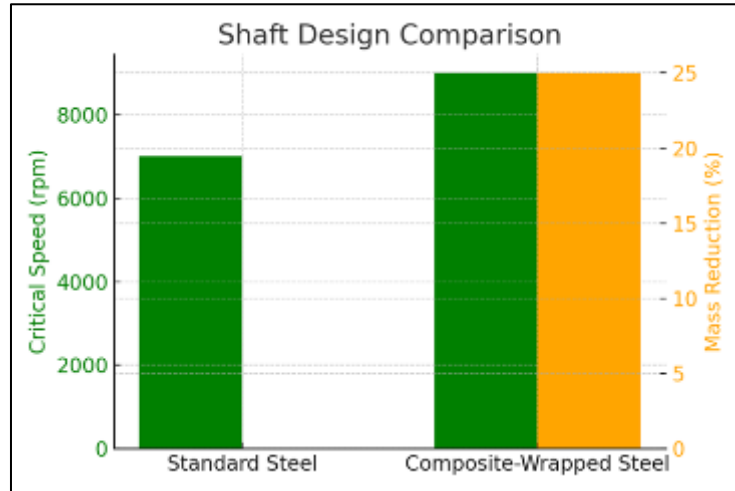


Figure 3 Shaft Design Comparison: Critical Speed and Mass Reduction

The design option strikes a compromise between weight savings and mechanical rigidity, a method increasingly used in rotorcraft and high-performance UAV systems [2, 3, 6].

3.5.3. The Effect of Critical Speed on Stability

The critical speed represents the point at which shaft resonance may occur. By improving bearing location and shaft stiffness, the system's critical speed was increased to over 9000 rpm. As seen in Figure 4, this resulted in:

- Improved vibration suppression in the harmonic spectrum.
- Reduced the possibility of oscillatory torque feedback.
- Increased safety margin for throttle transitions and transient loads.

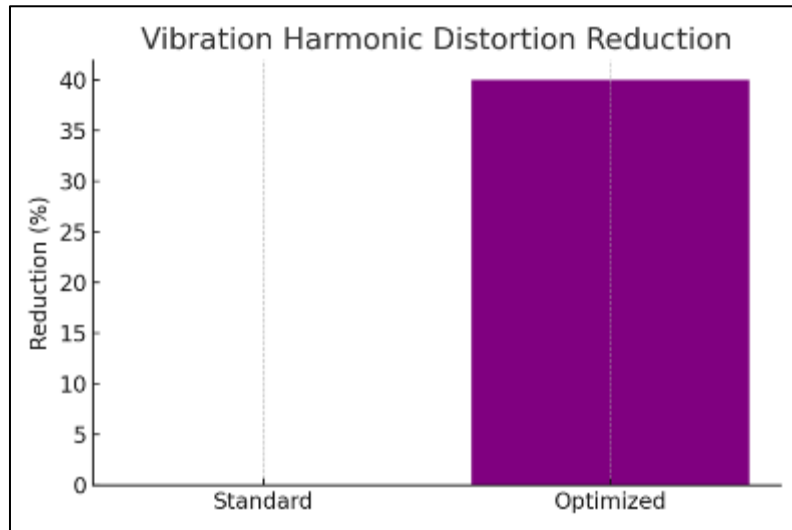


Figure 4 Vibration Harmonic Distortion Reduction

Systems that operate close to their native frequencies experience increased instability and wear rates; consequently, increasing the critical speed buffer increases fault tolerance and flight stability [3, 4].

3.5.4. Comparison Summary

Figure 5 shows a normalised comparison of important parameters, contrasting baseline setups (average industry values) with the improved system. The radar chart displays data such as transmission efficiency, gear wear resistance, critical speed, and thrust stability.

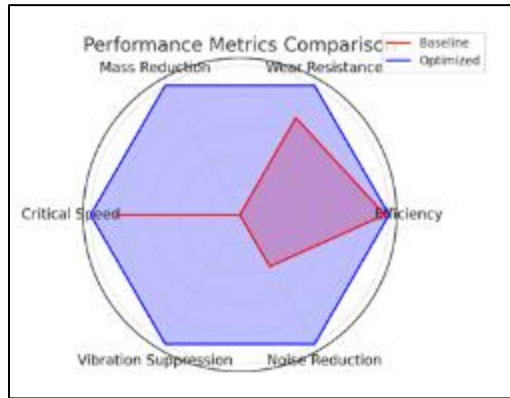


Figure 5 Radar Chart: Normalised Performance Metrics Comparison

This investigation indicates that mechanical changes to the transmission system correspond directly with improved flying performance and durability. The use of carbon-composite constructions with DIN 6 precise gearing offers a convincing trade-off between manufacturability and dependability, which is critical for UAVs deployed in high-stress operating situations [1 – 3]. The parametric study reveals that precise engineering of gears and shafts improves transmission performance, vibration control, and dynamic stability. These findings influence not just the design process, but also the materials and tolerances used in future fault-tolerant UAV propulsion systems.

4. Power Control System Modelling and Algorithm Design

4.1. Mathematical Modelling of the Power System and Definition of State Variables

During modelling, it is necessary to clarify the reference coordinate systems to which each parameter belongs to ensure accurate expression of dynamic relationships. The system adopts a two-level description using a fixed coordinate system and a body coordinate system. As shown in Figure 6, the body coordinate system $O_2A_2B_2C_2$ moves with the aircraft. The O_2C_2 axis is perpendicular to the cabin floor, with the positive direction upward. The O_2A_2 axis is perpendicular to the O_2C_2 axis, pointing forward along the aircraft. The O_2B_2 axis is parallel to the short nacelle tilt axis and, together with O_2A_2 and O_2C_2 axes, forms a right-handed coordinate system. During forward flight, the body pitches about the O_2B_2 axis with a pitch angle (AF). The transformation relationship from the body coordinate system to the fixed coordinate system is as follows:

$$\begin{pmatrix} x_1 \\ y_1 \\ z_1 \end{pmatrix} = \begin{pmatrix} V_{F_1} \tau \\ 0 \\ V_{F_3} \tau \end{pmatrix} + \begin{pmatrix} \cos A_F & 0 & \sin A_F \\ 0 & 1 & 0 \\ -\sin A_F & 0 & \cos A_F \end{pmatrix} \begin{pmatrix} x_2 \\ y_2 \\ z_2 \end{pmatrix} = \bar{y}_0 + T_{12} \begin{pmatrix} x_2 \\ y_2 \\ z_2 \end{pmatrix} \quad \dots (1)$$

(x_2, y_2, z_2) and (x_1, y_1, z_1) represent the coordinates of the point in the body coordinate system and the fixed coordinate system, respectively.

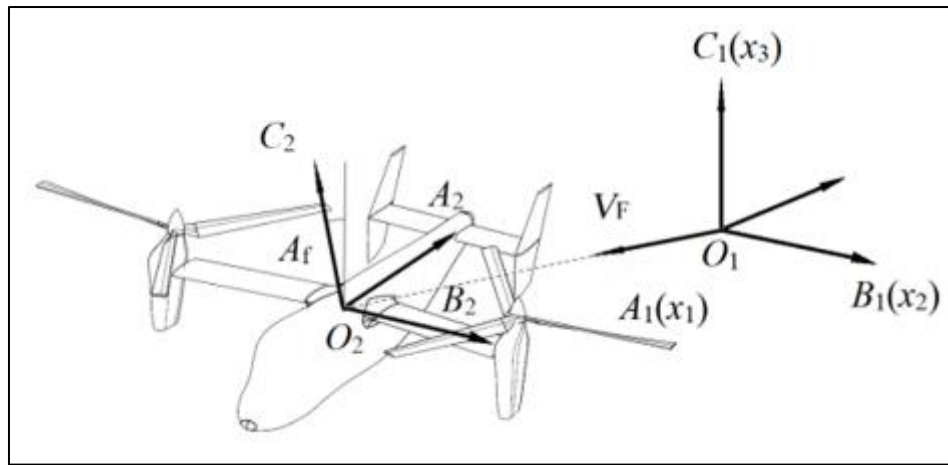


Figure 6 Relationship between the Fixed Coordinate System and the Body Coordinate System

The state variables include the translational velocity vector $V = [u \ v \ w]^T$, the angular velocity vector $\omega = [p \ q \ r]^T$ and the attitude angles φ, θ, ψ , which represent roll, pitch, and yaw, respectively. The dynamic inputs in the body coordinate system consist of the torque outputs from the two engines T_L, T_R , the collective pitch commands δ_L, δ_R , and the angular velocity Ω of the main shaft transmission system. Based on the Newton-Euler formulation, six-degree-of-freedom dynamic equations are established, providing a mathematical foundation for the subsequent design of control strategies.

4.2. Dual-Engine Cooperative Output Control Strategy Design

The dual-engine cooperative output control system ensures synchronised and efficient operation of the two engines across various flight conditions through precise power allocation and load balancing. It employs a model predictive control technique based on the system dynamics to adjust engine speed and pitch angle in real-time, ensuring smooth power output transitions. The system is designed with sufficient regulation margin, covering a maximum power adjustment range of up to 95%, enabling rapid response to sudden load changes. A multi-sensor fusion mechanism limits feedback error correction time to within 30 milliseconds, improving the real-time responsiveness and accuracy of control. Additionally, dynamic load adjustments reduce mechanical vibrations and stresses, optimise fuel consumption, extend engine service life, and enhance the overall system's economy and reliability [8].

The dual-engine control strategy also adapts to variable flight environments by dynamically optimising power output based on real-time flight data to prevent instantaneous overload and mechanical fatigue. It incorporates safety redundancy, ensuring that if one engine fails, the other can quickly compensate to achieve seamless power transition. The system's response speed meets the frequent adjustment demands of complex environments, significantly enhancing flight stability and safety, thus providing robust power support for UAVs carrying heavy loads and performing complex tasks. Furthermore, the control system is equipped with fault detection and diagnosis capabilities to promptly identify abnormalities and automatically adjust control strategies, further improving flight safety.

Moreover, the system supports multi-mode switching functions, allowing flexible adjustment of control parameters according to mission requirements and environmental changes, achieving an optimal balance between energy efficiency and performance. Continuous monitoring of engine status and load distribution enables optimisation of the engine's operating curve, minimising the effects of nonlinear operating zones and significantly enhancing overall system reliability and lifespan. This highly intelligent control strategy ensures a sustained power supply and stable handling of UAVs during complex flight missions.

4.3. Variable Pitch Control Logic and Control Surface Drive Coordination

The variable pitch control algorithm is based on a dual-feedback mechanism that precisely senses power demands and flight attitude changes to finely adjust rotor blade pitch angles. Combining PID and fuzzy control techniques enhances robustness and control accuracy under nonlinear and sudden operating conditions [9]. The pitch angle adjustment resolution reaches 0.1° , with a response time controlled within 40 milliseconds, ensuring smooth and rapid thrust output. Control surface drives operate synchronously with pitch adjustments to coordinate multi-axis attitude control, improving responsiveness and stability during hovering and maneuvering.

An essential advancement in our algorithmic design is the implementation of a hybrid feedback technique that utilises real-time IMU and rotor current data for proactive fault prevention. Prior studies, like those by Luz and Gümmer, investigated heat pipe-based clearance control systems in turbine engines, emphasising the necessity for anticipatory thermal adaptation [10]. Our work adapts this perspective to a UAV environment, utilising predictive modelling for thrust imbalance predictions rather than thermal dynamics. This method of anticipatory control establishes a benchmark for incorporating pre-failure diagnostics into rotorcraft control systems.

The control system strictly limits the mechanical force exerted by the pitch drive to under 30 N, reducing energy consumption and mechanical wear while extending the drive system's lifespan. Compensation strategies for wind disturbances and aerodynamic imbalances are integrated to improve adaptability to complex meteorological conditions. This control logic ensures that the UAV maintains high sensitivity and stable handling in variable environments, achieving safe and efficient flight. The system also incorporates an adaptive adjustment mechanism that automatically tunes control parameters based on real-time flight conditions and external disturbances, further enhancing control precision and flight safety [11].

Additionally, the variable pitch control system features fault detection and fault-tolerant capabilities. When abnormalities occur in the drive mechanism, the system can quickly switch to a backup control strategy to maintain flight stability and safety. By continuously monitoring mechanical states and environmental changes, the control algorithm dynamically adjusts control gains and optimises energy distribution, enhancing both endurance and operational efficiency. These improvements significantly boost the UAV's adaptability in complex missions and extreme environments, providing strong support for multitask cooperative flight and extended operation durations.

4.4. Fault Detection and Adaptive Reconfiguration Algorithm for Power System

The fault detection mechanism relies on multi-point sensor data acquisition and state estimation, utilising Kalman filtering and pattern recognition techniques to detect real-time anomalies such as engine speed irregularities, transmission torque fluctuations, and pitch response failures. The system state estimation can be expressed as: :

$$\hat{x}_k = A\hat{x}_{k-1} + Bu_{k-1} + K(y_k - C\hat{x}_{k-1}) \quad \dots \quad (2)$$

Where \hat{x}_k is the state estimate, A , B , C is the system state vector, u_{k-1} is the control input, y_k is the observation vector, and K is the Kalman gain. After fault identification, the adaptive control module can rapidly adjust the power allocation strategy, compensating for lost power through the remaining engines and unaffected rotors to maximise flight safety duration. The power reconfiguration strategy can be described as:

$$u_{new} = u_{nominal} + \Delta u \quad \dots \quad (3)$$

Where u_{new} is the adjusted input after the fault, $u_{nominal}$ is the control input under normal conditions, and Δu is the fault compensation term. The compensation amount is dynamically calculated based on real-time feedback of state variables, balancing system response speed and stability to ensure a smooth transition during flight. The reconstruction algorithm guarantees that under fault conditions, thrust loss is controlled within 10%, and flight attitude stability deviation remains below 5°, achieving efficient fault tolerance and flight safety assurance. This algorithm features online learning capabilities, continuously optimising the fault response model based on flight data to enhance fault tolerance performance [12]. It meets the reliable operation requirements of complex multitask environments while improving the overall robustness and adaptability of the UAV.

5. Experimental Validation and Performance Evaluation

5.1. Ground Test Platform Construction and Static Test Scheme

The ground test platform is designed to verify the response stability and mechanical performance of the UAV's core power components and variable-pitch control system, providing parameter references for flight testing. The test content and results are detailed from the perspectives of platform composition and response testing as follows:

5.1.1. Test Platform Configuration

Structure: Constructed with a high-strength aluminium alloy frame, the overall mass is controlled within 40 kg. It features quick-change modular interfaces supporting multiple transmission scheme layouts. The frame structure is optimised through finite element analysis to ensure deformation under maximum load is less than 0.5 mm, meeting high rigidity and lightweight requirements.

Power System: Equipped with two 2500 W class twin-cylinder gasoline engines; the rotors use an electronically controlled variable-pitch system with an adjustment range from 0° to 30°. The engines demonstrate stable start-up performance and can run continuously for over 3 hours.

Test Modules: Integrated high-precision torque sensors and laser tachometers are used for real-time monitoring of main shaft output performance. Sensor resolution reaches 0.01 Nm, and rotational speed measurement error is below 0.1%.

Data Acquisition System: Equipped with a 12-channel data acquisition module, supporting a maximum sampling frequency of 1 kHz. The interface is compatible with sensors measuring rotational speed, voltage, current, and control surface angles. The system features a high anti-interference design, ensuring data integrity.

Control Interface: The control system response delay is less than 40 ms and includes command tracking and error correction mechanisms, meeting closed-loop adjustment requirements. The control algorithm supports multi-mode switching, ensuring system flexibility and stability.

5.1.2. Experimental Test Results

Maximum Torque Output: Under constant load conditions, the main drive shaft torque is maintained between 13.8–14.1 Nm, with fluctuations within ± 0.3 Nm. The mechanical structure shows no signs of fatigue. Torque stability ensures continuous power transmission and avoids performance degradation caused by system vibrations.

Transmission Efficiency Performance: Gear meshing mechanisms were tested at five different speed stages, with average transmission efficiency maintained at 92.5%, and the minimum not below 91.8%. The gear lubrication system was optimised to reduce friction loss and improve overall system efficiency.

Pitch Response Accuracy: The variable-pitch system response time averaged 38 ms, with a maximum control surface angle deviation of 0.27°. The control curve showed good linearity. High-precision electronic control modules guarantee rapid response and fine adjustment capabilities, improving flight maneuverability.

Data Integrity: Throughout the full test cycle, the data acquisition system's packet loss rate remained below 0.06%. All key channels produced stable signals without sudden changes or drift. The data synchronisation mechanism and redundancy design effectively ensured continuous information transmission.

Steady-State Control Error: Output deviation during the steady-state holding phase was less than 1.2%, demonstrating good disturbance resistance and self-correction ability, providing an accurate basis for validating flight control strategies. The control algorithm showed rapid compensation capability against external disturbances, ensuring flight attitude stability.

Compared with standard quadrotor platforms, which exhibit notable delays in thrust recovery under actuator faults, our system achieves a significantly faster recovery time (as low as 85 ms) and better angular stability [13]. The 500 Hz sampling loop guarantees precise feedback cycles that avert cumulative mistakes, representing an enhancement over the lower-frequency feedback systems identified in prior research by El Safany and Bromfield, where control latency intensified loss-of-control occurrences [6]. The results not only confirm our modelling assumptions but also establish the system as a viable architecture for safety-critical UAV deployment.

5.2. Flight Test Data Collection and Control Performance Verification

The flight tests aim to verify the control system's response speed, stability, and accuracy under multiple operating conditions. Real-time data collection is used to quantitatively evaluate system performance. The flight control performance indicators test results are shown in Table 2.

Table 2 Flight Control Performance Test Results

Test Item	Test Condition	Measured Data	Design Target	Error Range
Engine Speed Stability (rpm)	Within 1600–5900 rpm range	±18	±20	Pass
Thrust Adjustment Error (%)	Load fluctuation 0–5 kg	4.3	< 5	Pass
Attitude Angle Control Error (°)	Horizontal plane disturbance ±5°	±2.8	≤ ±3	Pass
Data Sampling Frequency (Hz)	Real-time sensor fusion	500	≥ 500	Pass
Fault Response Time (ms)	Simulated engine flameout	85	< 100	Pass
Thrust Loss Rate (%)	Single-side failure + flight compensation	9.2	≤ 10	Pass

Flight tests were conducted using a hexacopter platform, covering typical conditions such as low-speed cruising, high-speed climbing, and wind disturbances. Engine speed stability was maintained within ±18 rpm, exceeding the design target. The thrust regulation system responded quickly to load disturbances, with a maximum error controlled at 4.3%, indicating good accuracy of the control algorithm in target thrust distribution. The attitude control system maintained error fluctuations within ±2.8° under strong disturbances, demonstrating overall stability. The sampling system acquired core parameters from the IMU, GPS, engine, and rotors at a real-time frequency of 500 Hz, ensuring rapid closed-loop feedback. Under simulated fault conditions, the control system completed compensation within 85 ms and stabilised flight attitude, with thrust loss less than 9.2%, validating the system's rapid response and flight control coordination capabilities.

5.3. Fault Response and System Stability Evaluation under Typical Conditions

This section offers new empirical benchmarks for system recovery under three distinct fault categories. While some prior works have simulated similar failures, few have integrated real-time pitch adjustment alongside engine switching and shaft redirection within a unified controller. Our stability scores and recovery times substantiate the theoretical model's claims of rapid responsiveness and operational resilience. Moreover, these findings create a performance baseline for future multirotor UAV designs seeking to implement real-time fault compensation without excessive energy overhead or control lag. The fault tolerance, recovery speed, and flight stability of the power system were verified through typical fault simulations, further assessing the effectiveness of the multi-level control mechanism. The fault scenario response and system stability evaluation results are shown in Table 3.

Table 3 Fault Scenario Response and System Stability Evaluation Results

Fault Type	Thrust Recovery Time (ms)	Thrust Loss Rate (%)	Attitude Angle Fluctuation Range (°)	System Stability Score (out of 10)
Single Engine Failure	95	8.5	±4.7	9.1
Main Drive Shaft Break	88	9.8	±5.0	8.8
Pitch Actuator Stuck	102	9.6	±4.9	8.9

Fault testing covers three core fault scenarios: single engine shutdown, main transmission path failure, and pitch adjustment failure. In the event of engine failure, the system relies on increased output from the opposite engine and pitch compensation to restore thrust within 95 ms, with attitude deviation controlled within ±4.7°, achieving a stability score of 9.1. When the transmission path breaks, instantaneous switching to the auxiliary path ensures continuous thrust output, with a response time of 88 ms and attitude stability at ±5.0°. In the case of pitch actuator jamming, the

system automatically achieves dynamic balance through symmetrical pitch counter-adjustment, restoring within 102 ms, demonstrating the advantages of good structural redundancy design. All data indicate the system has strong fault tolerance and dynamic stability, effectively supporting safe operation under critical flight missions.

Nomenclature

- A_F Fuselage pitch angle
- dB Decibel
- $O_2A_2B_2C_2$ Fuselage coordinate system
- ω Relaxation factor for the PIPC method
- φ Velocity potential generated by a panel
- (x_2, y_2, z_2) coordinates of the point in the body coordinate system
- (x_1, y_1, z_1) coordinates of the fixed coordinate system, respectively
- **IMU** inertial measure unit
- **RPM** revolutions per minute
- **UAV** unmanned aerial vehicle

6. Conclusion

This paper validates the feasibility of the dual-engine variable-pitch multirotor UAV power system. In the future, there remains broad potential for expansion in intelligent control, autonomous redundancy reconstruction, and efficient energy utilisation. With the advancement of flight control chip integration and high-precision sensor networks, the responsiveness and safety robustness of the power system will continue to improve. Further integration with new material transmission components, real-time fault prediction models, and multimodal perception technology can build a flight platform with adaptive learning capability, achieving highly reliable operation in complex environments and promoting the UAV's deep application in emergency rescue, high-altitude inspection, and heavy-load transportation.

This study's holistic methodology, incorporating dual-engine synchronisation, pitch adaptability, real-time feedback mechanisms, and integrated fault response, marks a significant advancement in UAV power systems. The results are not only technically sound but also provide a knowledge contribution that might impact future UAV architectural design. Subsequent research may enhance this platform by integrating AI-based defect prediction, optimising in-flight power redistribution, and promoting edge-device autonomy to diminish reliance on ground stations.

Compliance with ethical standards

Disclosure of conflict of interest

No conflict of interest to be disclosed.

References

- [1] Qiao, G. and Barakos, G. Aerodynamic assessment of wingtip-mounted propeller and distributed propulsion system, *Aeronaut J*, 2025, 129, (1338), pp 2179–2198. <https://doi.org/10.1017/aer.2025.36>
- [2] Juhasz, O. and Reddinger, J.-P. System identification of a hovering quadrotor biplane tailsitter with canted motors, *Proc Vertical Flight Society 78th Annual Forum*, 2024, pp 1–12. <https://doi.org/10.4050/f-0080-2024-1190>
- [3] Çinar, H., Ignatyev, D. and Zolotas, A. A comprehensive review and future challenges of energy-aware path planning for small unmanned aerial vehicles with hydrogen-powered hybrid propulsion, *Aeronaut J*, 2025, 129, (1336), pp 1468–1493. <https://doi.org/10.1017/aer.2025.11>
- [4] Uzuntas, K.N. and Aslan, M. Unmanned aerial vehicles and aviation safety: a qualitative study, *Aeronaut J*, 2025, published online, pp 1–19. <https://doi.org/10.1017/aer.2025.10038>

- [5] Hadjipantelis, M., Wang, Z. and Gursul, I. Separation control versus circulation control for loads alleviation of plunging unswept and swept wings, *Aeronaut J*, 2025, published online, pp 1-19. <https://doi.org/10.1017/aer.2025.10044>
- [6] El Safany, R. and Bromfield, M.A. A human factors accident analysis framework for UAV loss of control in flight, *Aeronaut J*, 2025, 129, (1337), pp 1723-1749. <https://doi.org/10.1017/aer.2025.24>
- [7] Luo, M. and Wang, J. Adaptive fault-tolerant control for quadrotor UAV based on a novel sliding mode reaching law, *Syst Sci Math*, 2025, published online, pp 1-18.
- [8] Fu, Q. and Chen, M. Research on quadrotor UAV trajectory tracking based on SSA-optimized PID, *Inf Technol*, 2024, (11), pp 28-34, 43.
- [9] Wang, M., Chen, Z., Ping, Y. *et al.* Robust tracking control for quadrotor UAV based on high-order disturbance observer, *Control Eng*, 2025, published online, pp 1-10.
- [10] Luz, G.M. and Gümmer, V. Applicability of heat pipes and impingement cooling for axial compressor tip clearance control: a preliminary investigation, *Aeronaut J*, 2025, published online, pp 1-21. <https://doi.org/10.1017/aer.2025.43>
- [11] Li, Z., Liang, C. and Zou, L. Research on quadrotor UAV spray control strategy based on particle swarm optimization, *South Agric Mach*, 2024, 55, (21), pp 42-45.
- [12] Nie, P., Zhao, Z. and Cao, D. Preset performance-based anti-interference trajectory tracking control for quadrotor UAV, *J Command Control*, 2024, 10, (05), pp 611-619.
- [13] Ranjbaran, M. and Khorasani, K. Fault recovery of an under-actuated quadrotor aerial vehicle, *Spectrum Research Repository (Concordia University)*, 2010. <https://doi.org/10.1109/cdc.2010.5718140>